Mineralogical Magazine, April 2003, Vol. 67(2), pp. 183–204

Identification and characterization of radioactive 'hot' particles in Chernobyl fallout-contaminated soils: the application of two novel approaches

J. A. ENTWISTLE[1], A. G. FLOWERS[2], G. NAGELDINGER[2] AND J. C. GREENWOOD[3]

[1] Division of Geography and Environmental Management, Northumbria University, Lipman Building, Newcastle upon Tyne, Tyne and Wear NE1 8ST, UK
[2] School of Life Sciences, Kingston University, Penrhyn Road, Kingston upon Thames, Surrey KT1 2EE, UK
[3] NERC ICP Facility, Kingston University, Penrhyn Road, Kingston upon Thames, Surrey KT1 2EE, UK

ABSTRACT

The Chernobyl accident in 1986 resulted in the widespread identification of the post-accident presence of radioactive (or 'hot') particles across large areas of Eastern and Central Europe. Such particles arise from direct deposition and also from condensation and interactions on particle surfaces during and following the deposition of soluble fallout. Identification of the presence and nature of hot particles is necessary in order to determine the long-term ecological impact of radioactive fallout. This paper describes several techniques for the identification and characterization of hot particles in soil samples from Belarus. In addition to new results from the use of gamma spectrometry, we include two novel instrumentation approaches that have been developed and applied to Chernobyl fallout-contaminated soils. The first, 'differential' autoradiography, utilizes a photographic film sandwich to characterize the nature of the ionizing radiation emitted from samples. In this paper we show that differential autoradiography can not only identify hot particle presence in soil, but can also determine the dominant radionuclide in that particle. The second approach, sector field ICP-MS (ICP-SFMS), can provide rapid, high-precision determination of the actinides, including the transuranic actinides, that characteristically occur in hot particles originating from weapons fallout or fuel matrices. Here, ICP-SFMS is shown to yield sufficiently low detection limits for plutonium isotopes (with the exception of ^{238}Pu) to enable us to confirm negligible presence of plutonium in areas outside the Chernobyl exclusion zone, but with high levels of fission-product contamination.

KEYWORDS: Chernobyl, autoradiography, actinides, transuranics, sector field ICP-MS, soil, hot particles.

Introduction

RADIONUCLIDES in the environment are present in many different physical and chemical forms. Differing atomic or molecular size, ionic charge and density influence their transport, distribution and bioavailability. The type of radioactive fallout is closely connected to the form of the radioactive accident or incident. Nuclear weapon explosions can generate huge quantities of radioactive particulates or 'hot particles' (Edvarson *et al*., 1959; Adams *et al*., 1960). In nuclear power plants hot particles arise as small fragments of irradiated fuel or material (usually of steel origin) that have been neutron-activated (Charles, 1991). Hot particles can also be released during nuclear accidents (Bogatov *et al*., 1990; Mandjoukov *et al*., 1992). Hot particles are not exclusively of anthropogenic origin. For example, small grains of thorium-bearing and uranium-bearing minerals, which occur naturally in soil, may also be described as hot particles.

Despite the fact that hot particles have been studied since the 1940s, their radiological significance had been underestimated and they only became recognized in the literature as an

* E-mail: jane.entwistle@unn.ac.uk
DOI: 10.1180/0026461036720094

important form of radioactive contamination of the environment following the Chernobyl nuclear power plant (ChNPP) accident on 26th April, 1986 (Mandjoukov *et al*., 1992). The total mass of radioactive particulate material estimated to have been released to the atmosphere as a result of the disintegration of the nuclear fuel mass and condensation of evaporated products from 25th April to 5th May 1986 was 6000−8000 kg (Victorova and Garger, 1990). Transport of these particulates depended on weather conditions, particle properties and effective release height (Pollanen and Toivonen, 1994*a*).

The hot-particle contribution to the activity of the upper layers of soil samples within the 30 km exclusion zone was found to be 86−93% (Tcherkezian *et al*., 1994). Most of the particulate material was deposited within 20 km of the plant, but about a third was transported much further (Powers *et al*., 1987). Chernobyl-derived hot particles have been detected across Russia, Ukraine and Belarus, and have also been detected in a number of other countries such as Germany, Poland, Sweden, Finland and Greece (Pollanen *et al*., 1997; Bolsunovsky and Tcherkezian, 2001). Such particles were distributed non-uniformly over a vast area and as a result, many environmental samples such as soil, vegetation and food, were contaminated not only by the 'normal' fallout, consisting of finely dispersed radioactive aerosols, but also by one or more hot particles (Bunzl, 1997). Pollanen *et al*. (1997) modelled the potential deposition pattern of Chernobyl-derived particulates over the 10-day release period (25th April, 21.00, to 5th May, 24.00). The model output for the potential deposition area of particles 20 μm in aerodynamic diameter, originating from release heights of 400 and 700 m, shows potential deposition over large parts of the Ukraine and extending into SW and SE Belarus.

This paper describes several techniques for the identification and characterization of hot particles in soil samples from Belarus. It includes two novel approaches that have been developed in recent years. The first, 'differential' autoradiographic imaging (DAI), utilizes a photographic film sandwich to characterize the nature of the ionizing radiation emitted from samples. The second approach, sector-field inductively coupled plasma mass spectrometry (ICP-SFMS), can provide rapid, high-precision determination of the actinides, including the transuranic actinides (e.g. Boulyga *et al*., 2001; Taylor *et al*., 2001; Truscott *et al*., 2001), which characteristically occur in hot particles originating from weapons fallout or fuel matrices. Here we report the results of Pu determinations. This work is part of an investigation to increase our understanding of the distribution of radionuclides in agricultural areas of SE Belarus that received significant fallout following the Chernobyl accident. Our work focuses on geographical areas with known ^{90}Sr and ^{137}Cs contamination that have been taken out of habitation and agricultural use but are now being gradually returned to that use. In areas such as this, that potentially received both soluble and particulate fallout, it is essential to define the nature of the fallout. Unless this is well-characterized, model prediction of the dispersion, ecosystem transport and dose assessment will suffer from unacceptably large uncertainties (Salbu, 2000).

Radioactive 'hot' particles

Mechanisms of formation and properties of hot particles

The term 'hot particle' essentially denotes a small radioactive fragment. Tcherkezian *et al*. (1994) defined 'hot particles' as radioactive particulates of <100 μm in size, with an activity greater than 4 Bq. There has been a number of suggestions as to the possible mechanisms of formation of hot particles linked to the Chernobyl accident (after Sandalls *et al*., 1993; Nageldinger *et al*., 1999): (1) mechanical emission of high-temperature liquid droplets from molten fuel, that solidified soon after ejection from the reactor; (2) formation of aerosol droplets by nucleation of vapour at high temperatures, and subsequent solidification on cooling; (3) condensation of water vapour onto existing water-soluble aerosols to form aqueous liquid droplets and subsequent evaporation of the water; (4) ejection of agglomerates or inclusions present in the fuel prior to the accident; and (5) condensation and then chemical interaction on particle surfaces following the deposition of soluble fallout components.

Results obtained by a number of workers show that the two main categories of particles associated with the ChNPP accident are: (1) Irradiated fuel fragment particulates (the so-called 'standard' hot particles making up ~85% of the particles; Mandjoukov *et al*., 1992). These fuel fragments are particles of uranium oxide fuel containing abundant transuranic actinides (e.g. ^{238}Pu, ^{239}Pu, ^{241}Pu, ^{241}Am, ^{242}Cm, ^{244}Cm) and a range of non-volatile fission products (e.g. ^{95}Zr,

^{95}Nb, ^{141}Ce, ^{144}Ce; Broda *et al*., 1989; Mandjoukov *et al*., 1992; Sandalls *et al*., 1993). These particles were often depleted in the more volatile elements, such as Cs, and contain varying amounts of ruthenium (^{103}Ru and ^{106}Ru); (2) Mono- or bi-elemental particles containing predominantly Ru isotopes, as well as a range of non-radioactive elements (e.g. Fe, Ni, Mo) and little or no uranium fuel (Osuch *et al*., 1989; Sandalls *et al*., 1993).

Health effects and environmental significance of the presence of hot particles

The health effects of hot particles depend on the number of particles and their properties. Particle size and activity are the main factors affecting radiological hazard (Pollanen *et al*., 1997). Small particles (<10 μm) may enter the respiratory tract through inhalation, thereby enhancing the radiological health hazard, because once deposited in the lung, highly concentrated irradiation occurs in the location around the particle. The intensified dose rate in the vicinity of a hot particle may lead to a zone of dead cells several mm thick, while beyond this zone, cells receive sub-lethal doses with an increasing carcinogenic risk (Philipsborn and Steinhaeusler, 1988). Particles may be ingested when associated with food products (Larsen *et al*., 1992) although this is not likely to be a critical pathway. Surface depositions on the skin, of large and highly radioactive particles, may lead to occupational dose limits being exceeded in a relatively short time (Larsen *et al*., 1992; Pollanen and Toivonen, 1994b). Failure to recognize the presence of hot particles in a sample can have a number of serious consequences. Firstly, the activity of the sample may not be representative of other samples that are not contaminated by hot particles. Secondly, inaccurate dose assessments may result if the very high local radiation doses, observed if hot particles are inhaled or incorporated into the body, are not taken into account (Bunzl, 1997). Thirdly, the modelling of environmental pathways may produce misleading results if the form and availability of the radionuclides are not well characterized.

Hot particles show a different behaviour in the environment from activity released in a gaseous or aerosol form (Zheltonosky *et al*., 2001). These forms of particulate are important because of the long-term and changing nature of their radiological health hazard. Following the ChNPP accident, the majority of fuel fragments deposited on the soil remained whole for a number of years following the accident, but are now disintegrating (Sandalls *et al*., 1993). Indeed several workers have reported changes in the soil-to-plant transfer of some fission products as a result of time-dependent weathering processes (e.g. Krouglov *et al*., 1997). The large number of physically and chemically persistent fuel fragments deposited after the ChNPP accident, and different chemical forms of ^{137}Cs and ^{90}Sr in the fallout, seem to be the most significant factors to explain the radionuclide behaviour in the near-field zone around the reactor. Committed dose to individuals due to intake of ^{90}Sr in agricultural products will change over time, becoming more important than ^{137}Cs in areas with 'fuel-type' contamination (Krouglov *et al*., 1997).

Hot particles containing actinide and transuranic isotopes produce an increasing radiological hazard for several decades after the original deposition. This arises from the decay of the beta emitter, ^{241}Pu, to the longer half-life alpha emitter, ^{241}Am, and a consequential increased level of radiological hazard from isotopes with a mass of 241. This has lead to increased interest in determining the physical and chemical characteristics of the transuranic actinides in soils from Chernobyl fallout areas. This interest is emphasized in the recent report from the Belarus State Committee on the Chernobyl Accident (Chevchuka and Gurachevsky, 2001), which notes the increasing contribution, over the next decades, of ^{241}Am to the overall potential radiological hazard, and highlights the need for further research on the likely impact of this isotope on the population's radiological dose.

Techniques for identification and measurement of hot particles

The earliest techniques for hot particle detection utilized autoradiography. Ionizing radiation from hot particles causes spots to appear on photographic film. Sizes and density of blackening enable an approximate determination of the magnitude of radioactivity in the particle. This technique has been used extensively for the investigation of radioactive particulates and dust generated by nuclear test explosions (e.g. Mamuro *et al*., 1965). Recently, we have developed the application of this technique by using differential autoradiographic imaging (DAI) to distinguish between radioactive emissions of

different types and energies (Nageldinger, 1998). The application of this technique to soil containing Chernobyl fallout is described in this paper.

Chernobyl hot particles have also been collected and identified using a variety of unconventional techniques. Sticky tape has been used for the collection of hot particles (Mandjoukov *et al*., 1992). Larsen *et al*. (1992) carried out repeated division and gamma spectroscopy of samples for the detection of hot particles. Sequential precipitation of the fine-earth fraction of soil samples in heavy liquids has been applied by Tcherkezian *et al*. (1994). Bondarenko *et al*. (1996) developed image analysis of etched tracks at the surface of TASTRAC (CR-39 type) plastics; the activity, physical size and position of the hot particle on the surface of the plastic was calculated. On flat surfaces, such as air filters or roofs, hot particles can be detected and localized in many cases by scanning devices or autoradiography (Bunzl, 1997). Hot particles have also been investigated with scanning electron microscopy (Philipsborn and Steinhausler, 1988).

Gamma spectroscopy, whilst frequently employed for quantitative analysis of radioactivity in bulk samples, can also be used to identify the presence and activity of hot particles. If hot particles are present in the sample, an inhomogeneous activity distribution will occur. If the soil is mixed repeatedly in the sample-counting container, and its gamma-ray emission rate counted each time, the resulting frequency distribution of the counts will not be a normal distribution with a standard deviation equal to the inherent measurement error. For this reason, it is possible to detect the presence of one or more hot particles in such samples simply by testing at a given level of significance whether the total number of counts observed after each mixing belongs to the same Poisson distribution (e.g. Bunzl, 1998; Nageldinger *et al*., 1998*b*).

ICP-MS is one of the most suitable methods for the isotopic analysis of long-lived radionuclides at ultra-trace concentrations. This renders it particularly appropriate for analysing the actinide activity of soils containing hot particles. Although thermal ionization mass spectrometry (TIMS) is the 'classical' isotope measurement method, ICP-MS is proving to be an acceptable and cost-effective alternative (Morrow and Crain, 1998). In this paper we show that ICP-SFMS yields detection limits for Pu isotopes that are significantly below the concentration levels of environmental concern. This capability is of importance for ascertaining that only low levels of this carcinogenic transuranic actinide are present in areas outside the exclusion zone, where high levels of fission product contamination occur and which are under consideration for potential rehabilitation.

Sampling locations in southeast Belarus

Soil samples were collected from southeast Belarus at evacuated locations, including sites near to where land rehabilitation is in progress. These samples were obtained from soil profiles at three locations, during the period July 1996–July 2000 (Fig. 1). One location was within the 30 km zone surrounding the reactor, known as the exclusion zone. The other two locations were in the Gomel region, 170 km northeast of Chernobyl. The selected locations are within two of the main spots of contamination resulting from the Chernobyl accident, referred to by OECD as the Central Spot, and the Bryansk-Belarus Spot (OECD, 1995).

The exclusion zone location is part of the Central Spot, which was formed during the initial release of radioactivity from the Chernobyl nuclear power plant (ChNPP). Here, the surface deposition exceeded 1.5 MBq m^{-2}. The exclusion zone sampling site (EZ: sandy soil) is ~15 km north of the reactor (latitude 51º30.49′, longitude 30º1.17′). The selected sampling location is known for the occurrence of hot particles (Tcherkezian *et al*. 1994; Nageldinger *et al*. 1998*b*). In this area, hot particles contribute not less than 65% of the total activity (Tcherkezian *et al*., 1994). At this sampling site the integrated dose rate at 1 m above ground was 5.6±1.1 μSv h^{-1} on 9th July 1996.

The Gomel region sampling locations lie within the Bryansk-Belarus Spot centred 200 km north-northeast of the reactor. This spot was formed on 28−29th April 1986 as a result of rainfall. The ground deposition of ^{137}Cs was comparable to the levels in the Central Spot. The two sites we selected are referred to as Vetka-C (sandy-loam soil: located at latitude 52º39.67′, longitude 31º24.54′) and Vetka-D (organic soil: located at latitude 52º38.21′, longitude 31º26.58′). The integrated dose rate at 1 m above ground at these two sites was 2.2±0.3 μSv h^{-1} and 1.6±0.3 μSv h^{-1}, respectively, on 12th July 1996. In the sections below we show how gamma spectroscopy, DAI and ICP-SFMS have

FIG. 1. Site location map showing sampling locations EZ (Exclusion Zone: latitude 51°30.49′, longitude 30°1.17′) and Vetka (Vetka-C: latitude 52°39.67′, longitude 31°24.54′, and Vetka-D: latitude 52°38.21′, longitude 31°26.58′) in Belarus. Shaded regions have a ^{137}Cs ground deposition of >555 kBq m^{-2} (OECD, 1995).

been applied to the analysis of Chernobyl fallout-contaminated soil samples.

Hot-particle detection using gamma-radiation detection from repeatedly mixed samples

Gamma spectroscopy is frequently employed to determine the radioactive content of gamma-ray emitting isotopes in soil samples. The method is suitable for detection of important components of Chernobyl fallout, such as ^{137}Cs and ^{241}Am, that are gamma-ray emitters, but not for the significant long-lived ^{90}Sr radioisotope, which is a pure beta emitter. This section describes how the variable geometric efficiency of gamma-ray detection over the volume of a large sample can be used to determine the extent of the hot-particle content. The results presented here were obtained using the measurement and analysis technique developed by us and described in Nageldinger *et al.* (1998*b*). Bunzl (1998) details a similar technique. This measurement procedure has widespread practical application for detecting hot particles in large quantities of dust or dirt, e.g. in nuclear power plants. Estimation of the number and activity of hot particles present can be made, but only if the activity level of all particles is assumed to be similar.

Gamma spectroscopic method for hot-particle identification in sandy soils

Sandy topsoil (0−2 cm depth) samples, taken from the exclusion zone (EZ) and the Vetka region (Vetka-C) sampling sites, were investigated using a gamma spectroscopic method. The 661.66 keV gamma-ray associated with ^{137}Cs decay was chosen for the purpose of this procedure. At the time of measurement, in 1998, ^{137}Cs with a half life of 30.1 years contributed most of the gamma and the beta activity in the Chernobyl fallout contaminated soil. For this reason, ^{137}Cs has been observed extensively in studies on Chernobyl fallout. However, the effect of hot-particle content on the spectroscopic analysis of volume samples has generally been neglected.

Each soil sample was air-dried, passed through a certified laboratory test sieve of 850 μm aperture, dried in an oven for 2 days at 105°C, and placed in a wide mouth, non-sterile, cylindrical polysterol container. The soil sample was then shaken and stirred. A 'calculated ^{137}Cs specific activity', was determined for the reference date 1st January 1998. The activity of ^{137}Cs was determined using a high-purity germanium (HPGe) coaxial photon detector system. The dimensions of the crystal are 51.5 mm diameter

with a length of 52.0 mm. The endcap to crystal distance is 3 mm. The resolution (FWHM) at 1.33 MeV (^{60}Co) was 1.86 keV with a relative efficiency of 21.1%. The detector was placed in a lead shield 10 cm thick. The spectroscopic analysis of the net peak area together with the statistical uncertainty calculation was carried out using the Canberra Genie-PC Spectroscopy software system. A sample volume of 180 cm^3 was selected to optimize count time and to avoid pulse pile-up. The sample container was located directly on top of the detector endcap. The height of the container extended 75 mm from the detector end cap. This resulted in the difference in the detection efficiency for ^{137}Cs located at the top and bottom of this container being approximately a factor of 8 (Nageldiner *et al*., 1998*a*). Detection efficiency was derived using an homogeneous source with the same reference geometry. The reference geometry was produced through careful mixing and drying of a similar soil type with an aqueous solution containing a mixed radionuclide standard solution (ampoules A938/96-A960/96, 0.4± 0.001 Bq ml^{-1}, product code R08-04 obtained from the National Physical Laboratory, Teddington, Middlesex TW11 0LW, United Kingdom).

This shaking, stirring and measurement procedure was repeated 100 times for each sample. The background spectrum was recorded on a regular basis during this sequence of measurements. The quantity we describe as 'calculated activity' is obtained on the assumption that the source of ^{137}Cs is homogeneously distributed throughout the volume of the sample. The sequentially determined values of 'calculated activity' were plotted against the experiment number (Fig. 2*a*,*b*). In the 2 cm thick topsoils at sampling sites EZ and Vetka-C, the ^{137}Cs specific activity ranged between 100 and 130 kBq kg^{-1} dry mass. The statistical 2σ counting error on each determination was kept below 0.4%. The target counting error of 0.4% could be reached with a counting time of <20 min. If different spatial hot-particle distributions occur in the sample geometry, for repeated measurements, then variability in the 'calculated activity' in excess of the statistical counting error may be observed.

The data in Fig. 2 represent a sequence of repeated attempts to homogenize each sample. The fluctuations of the calculated activity can be seen (Fig. 2*a*,*b*) to be larger than the expected statistical counting error (indicated by error bars on each measurement in Fig. 2). Given the finely ground nature of the soil sample, the fluctuations are consistent with an inhomogeneous distribution of activity in the sample volume. We ascribe the inhomogeneity to the presence of localized concentrations of radioactivity within the sample, i.e. the presence of hot particles. In the case where a large number of radioactive particles is present in the sample geometry, the calculated activity should converge to a final value, within the measurement statistical error, during the process of repeated mixing. Lack of convergence confirms the assumption of an inhomogenous radioactivity distribution in the sample due to a lower number of hot particles. Later we quantify this number in relation to the results of a Monte Carlo simulation.

The calculated activities for the EZ topsoil vary between 101.6 and 113.4 kBq kg^{-1}. The Kolmogorov-Smirnov one-sample test was applied to decide how well the sample activity distribution fitted a normal distribution (at a significance level of 0.05). The test yields the statistical test parameter, D_{KS}, and a goodness of fit significance level α_{KS}. For the EZ topsoil, the determined activity distribution had a D_{KS} of 0.074 with a significance level, α_{KS}, of 0.64. This is confirmation of a normal distribution. For the Vetka-C topsoil, the calculated activities vary between 109.5 and 125.6 kBq kg^{-1}. The resulting activity distribution it is not normally distributed, as a D_{KS} of 0.161 was calculated, with a significance level α_{KS} of 0.011.

Hot-particle number, activity and distribution

The activity distribution of the fallout-contaminated EZ topsoil is normal; with a mean ^{137}Cs specific activity of 107 kBq kg^{-1} and a standard deviation of 2%, which is greatly in excess of the statistical counting error 0.4%. A Monte Carlo simulation (Nageldinger *et al*., 1998*a*) for this source-detector geometry has shown that the generated sample activity distributions are normal if the number of hot particles is larger than a certain limit, and assuming the same activity for every hot particle. This limit, in our case, was at ~50 hot particles (Nageldinger *et al*., 1998*b*). Even if the sample activity distributions are not normal for a small number of hot particles with the same activity, an inverse proportional relationship exists between the logarithm of the standard deviation and the logarithm of the particle number. This relationship can be used to

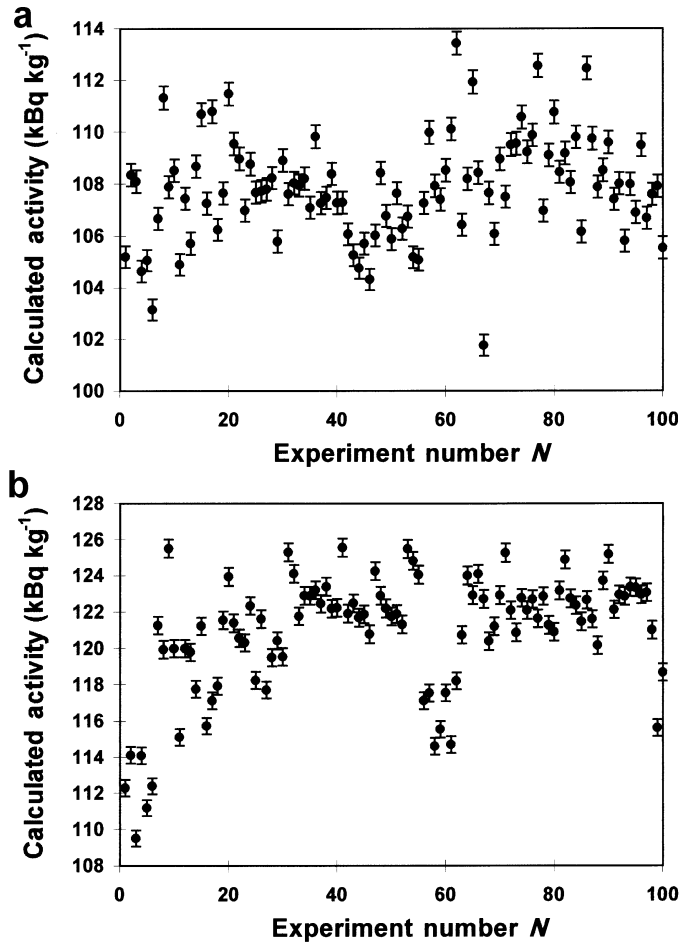

FIG. 2. Calculated specific activity (reference date 1st January 1998, determined assuming source homogeneity) *vs.* experiment number *N* (error bars indicate 2σ statistical counting error) for sandy topsoil originating (*a*) from the sampling site EZ (Exclusion Zone) and (*b*) from sampling site Vetka-C.

estimate the number of hot particles present, if the activity of all particles is assumed to be similar. In the case of the EZ sample, assuming that all the hot particles containing ^{137}Cs have a similar ^{137}Cs activity, our Monte Carlo simulations (Nageldinger *et al*., 1998*b*) indicate that 100 g of the soil sampled at site 'EZ' contains ~500 hot particles. The approximate activity of each of these particles is 20 Bq (as at 1st January 1998).

An estimation of the number and activities of hot particles present in the soil sampled from the Vetka region 170 km north-northeast of the ChNPP is difficult. The calculated activities for this sample ranged between 109.5 and 125.6 kBq kg^{-1}. The high Pearson skewness coefficient (−0.77) for this sample activity distribution, and the standard deviation of 2.8% are characteristic of either a small number of highly radioactive particles, or, a large number of particles of varied radioactivity. Hence, the number and activity of hot particles was not estimated for this sample, since the skewness of the distribution of the repeated spectroscopy activity measurements indicated that it was not justifiable to assume that most of the hot particles present had a similar activity.

Here we have shown that the distribution of hot particle activity may be more varied at the site 170 km from Chernobyl (Vetka-C), compared to that 15 km from the reactor (EZ). Care should be taken when soil sample activity levels are compared down a soil profile, particularly if

these are used to fit a radionuclide transport model. The soil sample activity error should include not only the statistical counting error and the error determined from the efficiency calibration, but also an additional radioactivity inhomogeneity error as described above. If no activity error is included (e.g. Belli and Tikhomirov, 1996; Sanzharova *et al*., 1996), it may be possible to obtain radioactivity depth distributions (soil activity profiles) by gamma spectroscopic techniques, which suggest a peak in the distribution. Care must be taken to ensure that this peak lies outside any measurement error that could arise from inhomogeneous hot-particle distributions in the measured samples for different soil layers.

This gamma-ray detection method gives a clear indication of any dominant presence of gamma-ray emitting hot particles. The method is not only applicable to small numbers of high-activity particles but also in cases when large numbers of low-activity (few Bq) particles are present in samples. In this latter case, long counting times may be necessary to ensure the statistical error of each measurement is significantly lower than the standard deviation of the activities obtained by repeated measurement of mixed samples. However, the method is inapplicable to pure beta emitters. In the next section we describe a method that enables identification of the presence of the pure beta emitter, ^{90}Sr, in hot particles.

Chernobyl fallout hot-particle characterization using differential autoradiographic imaging

Here we use the term 'differential autoradiographic imaging' (DAI) to refer to the technique of analysing ionizing radiation by use of a sandwich of layers of photographic film interspersed by phosphor screens. This technique extends conventional single layer photographic film techniques by using the different attenuation characteristics of different energies and types of ionizing radiation. It utilizes the phosphor screen layers to enhance the film exposure. The technique is capable of distinguishing between hot-particle radioactive emissions of different types and energies. In this section we describe how DAI can be utilized to indicate the dominant fission isotopic content and radioactivity of hot particles in radioactive contaminated soil.

The DAI sandwich, which we developed to locate and analyse hot-particle radioactivity in contaminated soil, is shown in Fig. 3. The sandwich is contained in a Kodak Biomax Cassette (a). Radiation from the soil sample (e), located in the frame (f) is incident sequentially on the films X, Y and Z, after sequentially passing through the phosphor screens (d) and (c), and also part of the light reflective material (b). Alpha particles, being short-range, will mostly affect film X, nearest to the soil sample. High-energy beta radiation, and also gamma radiation, may be detected on all three films.

The nature of the radioactive emissions can be distinguished by comparison of the exposure image obtained in each of the three films (X, Y and Z) for the same film location. Digital processing of the exposed film is used to convert the image into a two-dimensional array of greyscale pixels. It is then possible to characterize each pixel with a standardized numerical value of reflection density according to a standard Kodak 20 point grey scale (values 0.0 to 1.9) (Nageldinger *et al*., 1998*a*). These reflection

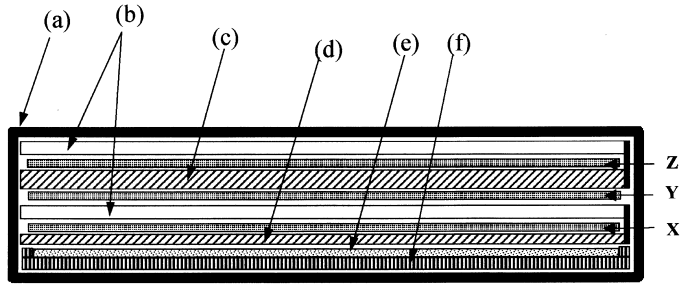

FIG. 3. Differential Autoradiographic Imaging (DAI-sandwich) Assembly: (a) Kodak BioMax^{TM} Cassette; (b) reflective surface of Kodak BioMax^{TM} TranScreen folder to which a low or high energy phosphor screen is hinged; (c) phosphor layer of ~0.165 mm on clear plastic backing of 0.102 mm thickness (high energy (HE) version); (d) phosphor layer of about 0.102 mm on clear plastic backing of 0.037 mm thickness (low energy (LE) version); (e) 1 mm soil layer; (f) soil frame; X, Y and Z - Kodak BioMax^{TM} MS X-ray film.

densities can then be compared between films. Figure 4 presents the reflection density value for each pixel on the Y film plotted against the X film value for the corresponding pixel for exposures to eight different radioisotopes. Here we refer to these scatter plots as 'pixel scatter plots' (PSPs).

The PSPs obtained using a DAI sandwich can be used to differentiate between beta emitters of

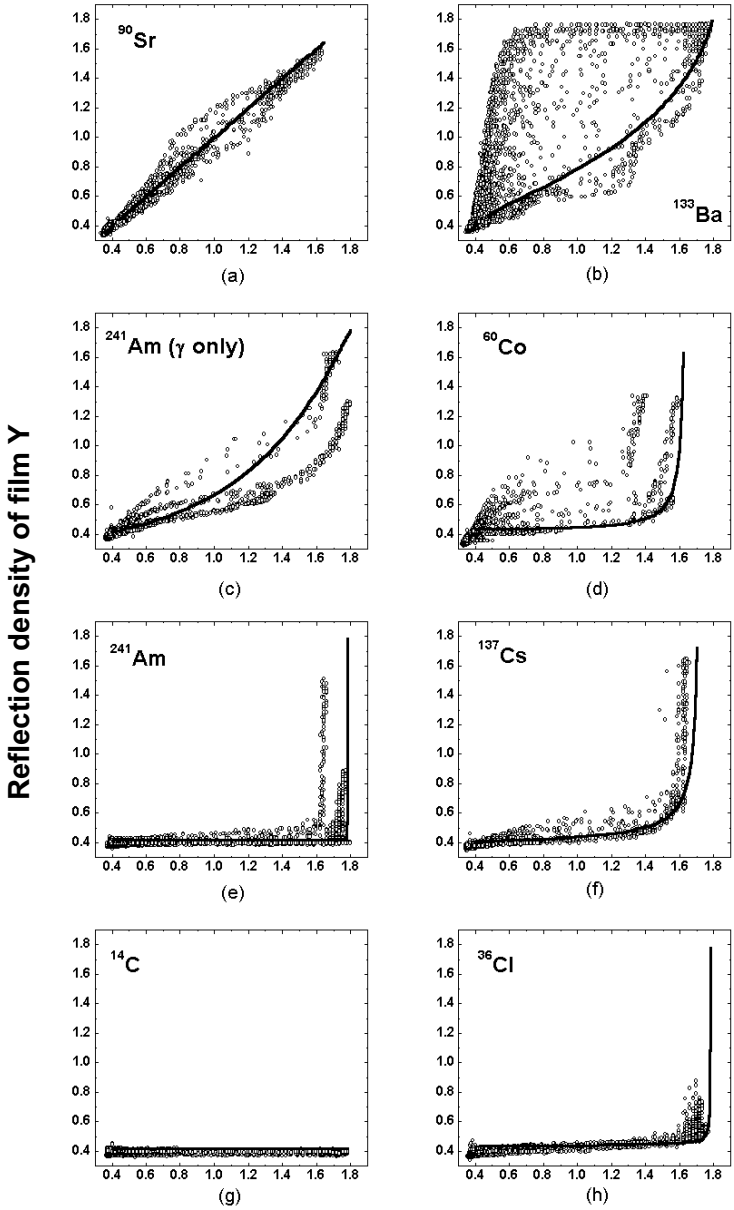

FIG. 4. Pixel scatter plots (PSPs) of the X and Y film reflection densities obtained from eight different single isotope sources of artificially created radioactivity spots (*a*–*h*). The solid line indicates the relationship between the reflection density of film X and film Y for idealized point sources, and is referred to as the 'maximum density scatter plot line' (MDSP).

different energies. Here we note that ^{90}Sr (half-life 28.6 years) is in equilibrium with its daughter ^{90}Y (half-life 2.67 days), in both the analysed soil samples and calibration standards. ^{90}Y has an emitted beta particle energy spectrum which extends up to an end-point energy of 2.28 MeV. This contrasts with the much lower end-point energies for beta emission from ^{90}Sr (0.546 MeV for 100% of decays), ^{137}Cs (0.511 MeV for 94.6% of decays, 1.17 MeV for 5.6% of decays), and ^{14}C (0.157 MeV for 100% of decays) (Longworth *et al*., 1998). It is this range of emitted beta particle energies, taken together with ^{137}Cs, also a gamma emitter, that enables the DAI technique to differentiate between the environmentally significant isotopes ^{137}Cs and ^{90}Sr/^{90}Y (in equilibrium). In this work, where reference is made to ^{90}Sr it is to be understood that this refers to ^{90}Sr/^{90}Y, in equilibrium.

Figure 4 illustrates radionuclide differentiation using the DAI technique. The solid line on Fig. 4*a*–*h*) indicates the relationship between the maximum reflection density obtained on film X and film Y for idealized point sources. Here we refer to this line as the 'maximum density scatter plot line' (MDSP). This line depicts the relationship between the maximum reflection densities, obtained by exposure of two of the films within the DAI sandwich, to a range of radioactive calibration standards. Each point along the curve relates to one specific rate of radiation discharge for the given radionuclide. Differentiation of alpha-emitting isotopes could not be achieved. This is because any significant occurrence of alpha-particle radiation will highly expose film X (the first film in the sandwich), but will not show up on film Y. Thus, although a significant presence of alpha emitters can be identified, the actinide isotopes, such as $^{235,\ 236,\ 238}$U, and the transuranic actinides, such as ^{237}Np, $^{236,\ 238,\ 239,\ 240}$Pu, ^{243}Am and ^{244}Cm, cannot be distinguished using this technique. This also occurs with low-energy pure beta emitters (e.g. ^{14}C) and in Fig. 4 the similarity between the ^{14}C PSP (g) and the ^{241}Am PSP (e) is evident. Fortunately, some alpha-emitting isotopes have accompanying gamma emission that enables these alpha/gamma emitters (e.g. ^{241}Am (c)) to be distinguished from low-energy pure beta emitters (e.g. ^{14}C (g)). Additionally, any dominant presence of isotopes that emit penetrating beta and/or gamma radiations will mask the presence of alpha emitters, since they will induce exposure in the Y and Z films.

In Fig. 5 we present the digitized images of the three developed DAI sandwich films following a 14 day exposure to a soil sample contaminated by Chernobyl fallout, that was collected at the exclusion zone site (location EZ, described above). The soil was dried for a period of two days at 105ºC in an oven, and roots and other plant parts were separated from the soil with a laboratory test sieve of 850 μm aperture. The soil (25 g) was placed in a 1 mm deep tray beneath the DAI sandwich. The dark spots originating from localized high density of radioactive emissions indicate the presence of hot particles.

Classification of the hot particle isotopic content of this sample was undertaken using two techniques of image analysis of the DAI sandwich films. We refer to these as 'Individual Spot DAI analysis' and 'Contrast Enhanced DAI'.

Individual spot DAI analysis of soil contaminated by the Chernobyl accident

The DAI technique was applied individually to two of the dark spots, which we infer to have formed by exposure to hot particles. These spots are identified in Fig. 5 as areas (a) and (b). The corresponding areas (a) and (b), in films X, Y and Z, were electronically cut out of the three autoradiograms, keeping size and position for each of the spots on the three films the same. The areas were then densitometrically evaluated to yield the PSPs shown in Fig. 6.

The application of Individual Spot DAI analysis requires comparison of the PSPs, with the form expected for radionuclides likely to be present in the sample. In the case of Chernobyl fallout, by the time this sample was analysed in 1998, the dominant radioisotopes could only be ^{137}Cs, ^{90}Sr or actinides. The shape of the PSPs indicates the presence of high-energy beta emitters suggesting it is appropriate to characterize the hot particles in terms of their ^{90}Sr or ^{137}Cs content. As particulates containing mainly ^{90}Sr or ^{137}Cs can also contain other isotopes, the term '^{90}Sr-dominated' or '^{137}Cs-dominated' is used to characterize identified particles, while recognizing the possible presence of lower-level activities of other isotopes.

Figure 6 indicates the MDSP for ^{90}Sr (bold line) and ^{137}Cs (dashed line). The PSP of area (a) follows the MDSP of ^{90}Sr whilst the PSP of area (b) follows an MDSP that is more indicative of a mixture of ^{137}Cs and ^{90}Sr. The DAI sandwich differentiates best between ^{137}Cs and ^{90}Sr using

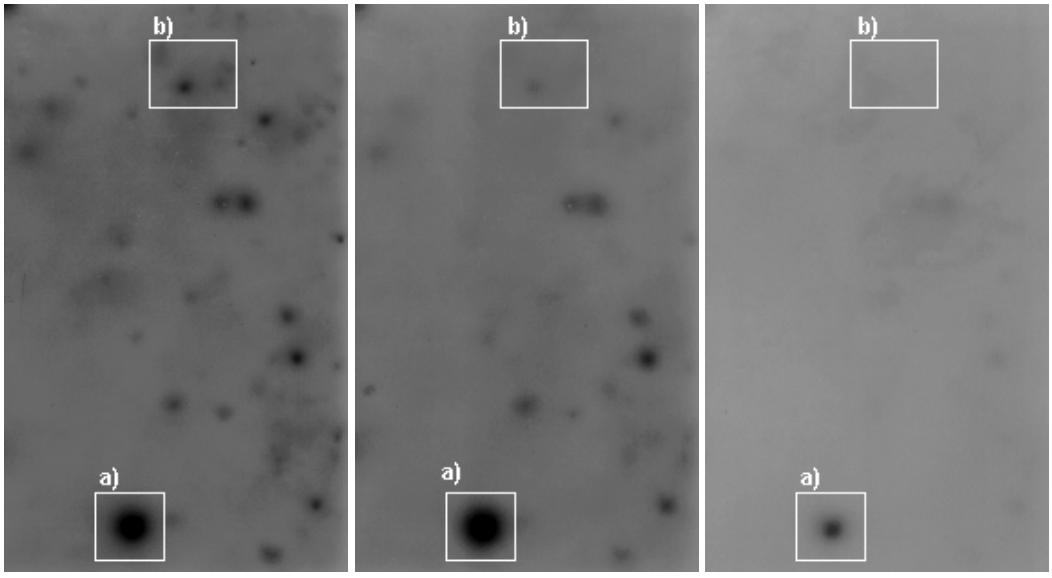

FIG. 5. Exposure of the DAI sandwich films, X, Y and Z, by hot-particle-contaminated soil (sampled 15 km north of the Chernobyl Nuclear Power Plant). The original film size is 85×110 mm^2. The exposure time was 14 days. Area (a) shows irradiation from a ^{90}Sr-dominated hot particle whereas irradiation in area (b) is caused by a ^{137}Cs-dominated hot particle.

the PSP produced by comparing reflection densities in films X and Y (Fig. 6*a* and *d*). The sample activity in this case was high enough to expose film Z after an exposure time of 14 days. This is illustrated for both areas (a) and (b) in the PSP obtained by comparing reflection densities on films X and Z, as shown in Fig. 6*b* and *e*. The PSP of films Y and Z, shown in Fig. 6*c* and *f*, is only of limited use for the differentiation of these two particles since the MDSPs for ^{90}Sr and ^{137}Cs are not easily resolvable.

The activity of the ^{90}Sr-dominated hot particle can be estimated by comparison of the film exposure density with films exposed to calibrated radioactive sources. Over a 14-day period an average surface exposure density equivalent to 2×10^5 beta discharges mm^{-2} was found to occur over the surface of area (a) (Fig. 5). Assuming that all the incident radiation that caused spot (a) originated from ^{90}Sr, and given that area (a) covers 116 mm^2, this indicates a total ^{90}Sr activity from the hot particle to be ~40 Bq.

Contrast-enhanced DAI

Films X and Y, as shown in Fig. 5, were transformed into a 'contrast-enhanced image' map of the autoradiograph. This involves transforming the 'original grey scale' using an 'applied grey scale'. This results in an image (Fig. 7) that is an image enhancement of the autoradiograph shown in Fig. 5. The enhanced image allows clearer identification of high-density exposure on the films, which we attribute to hot particles. This image can then be used to obtain a count of the numbers of hot particles.

Forty-seven hot-particle exposed spots could be identified from the 25 g sample of Chernobyl contaminated soil from site EZ (Fig. 7). Nageldinger *et al*. (1998*b*) estimated that ~125 hot particles (containing ^{137}Cs) were present in a similar 25 g of soil, taken from the same location. This estimate was made using the gamma spectroscopic shaking and measurement procedure outlined above. The difference is not necessarily a discrepancy, since a number of hot particles below the lower film exposure threshold of 3×10^4 total gamma discharges mm^{-2} (here, equivalent to 6 Bq per particle) are not detectable with autoradiographic methods using the 14-day exposure times utilized in this study.

Dense spots on film X that are caused predominantly by ^{90}Sr will have similar reflection densities on both films X and Y. A comparison of

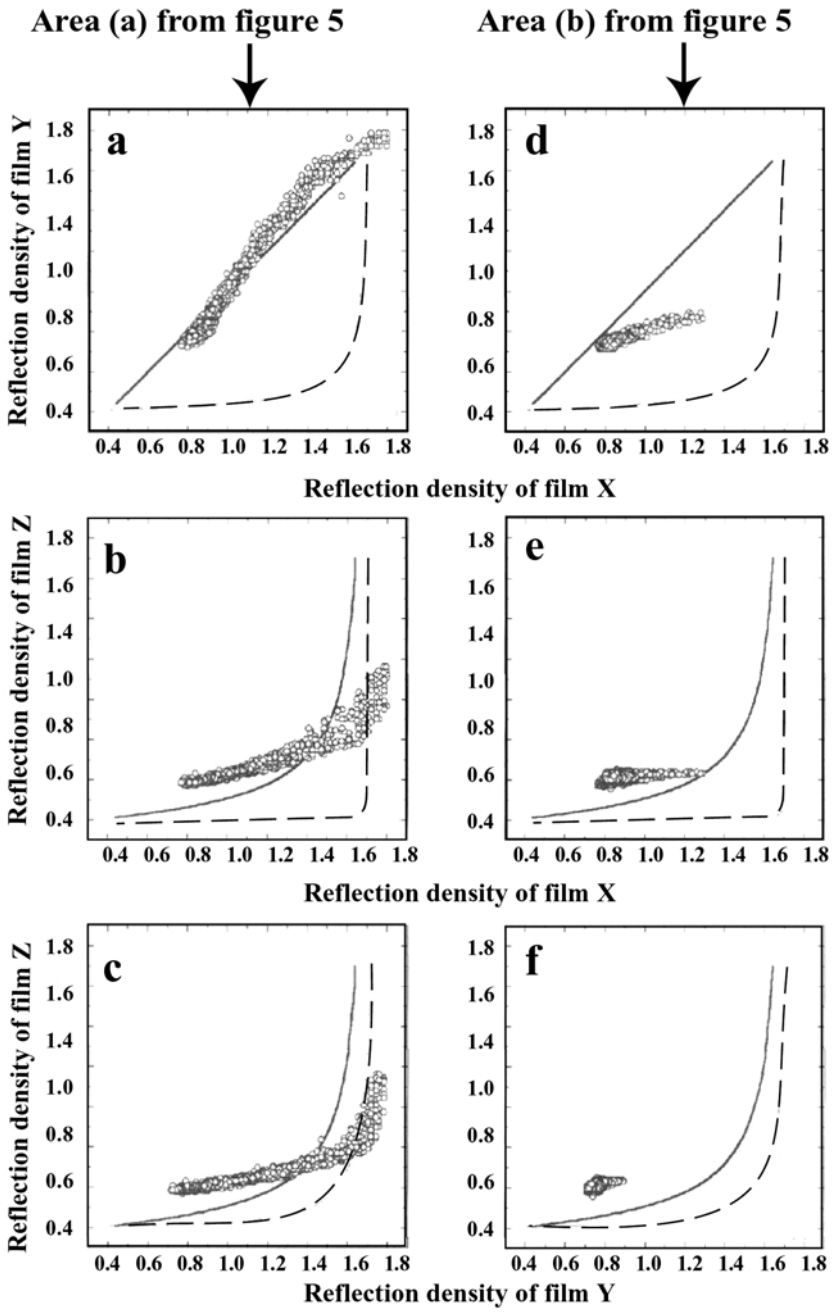

FIG. 6. Pixel Scatter Plot (PSP) generated from film X, Y and Z, shown in Fig. 5, for area (a) and (b). The bold line represents the Maximum Density Scatter Plot line (MDSP) for ^{90}Sr and the dashed line shows the MDSP for ^{137}Cs.

film X with film Y shows that only 6 out of the 47 hot particles identified on film X have a similar reflection density on film Y (Fig. 7). Therefore, these spots are likely to be dominated by ^{90}Sr emissions. Thus, in this sample, we identify a prevalence of ^{137}Cs-dominated hot-particle content over ^{90}Sr dominated hot-particle content. The cloudy regions on film X, e.g. that around hot

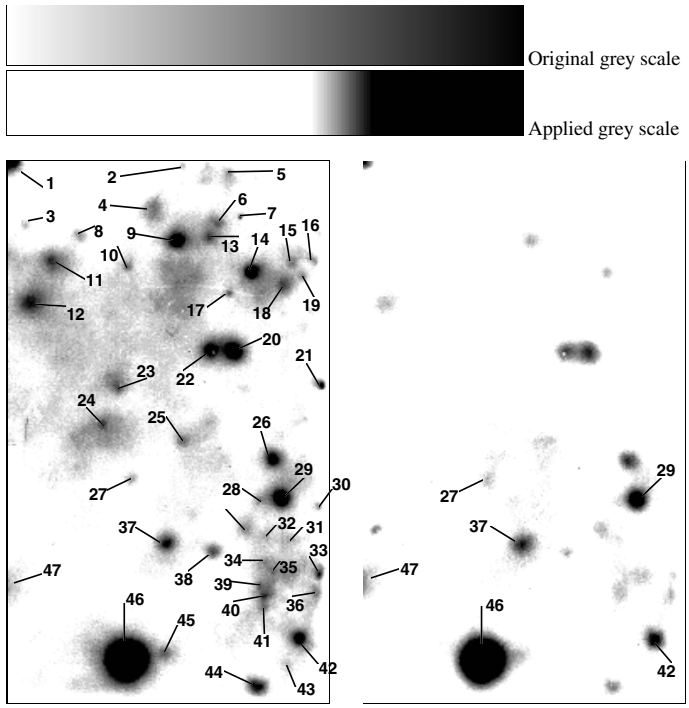

FIG. 7. Contrast-enhanced film X and Y of Chernobyl contaminated soil. The contrast enhancement was obtained by mapping the original reflection density values against the applied grey scale. The numbered spots on film X represent hot particles, whilst the numbered spots on film Y have been identified as ^{90}Sr-dominated hot particles.

particle 9 (Fig. 7) do not appear on Film Y. We suggest that these regions are caused by a homogeneous or diffuse type of radionuclide contamination rather than by hot particles. This region could not be attributed to either dominant ^{90}Sr or ^{137}Cs emissions, since the MDSP reflection density values are between those of ^{137}Cs and ^{90}Sr.

As mentioned previously, this method is not suitable for analysing actinide, including trans-uranic actinide, content. Hence we have applied ICP-SFMS to obtain an indication of the upper limits of Pu-bearing hot-particle content in our samples.

Chernobyl fallout hot-particle characterization using ICP-SFMS

Instrumentation, standards and reagents

Here we present an analysis of the Pu isotopic content of the soils sampled at location EZ, Vetka-C and Vetka-D. Isotopic measurements of these samples were obtained using an ICP-SFMS instrument (Axiom, Thermo-Elemental, UK) in low-resolution mode (mass resolution of 450), fitted with a single detector. An ion source (the plasma), sampling interface and a lens system are utilized, as in traditional quadrupole-based instruments. Ions are transferred from the plasma, through an entrance slit, accelerated in an electric field and injected perpendicularly into a magnetic sector field. The instrument can be operated at low mass resolution (slits fully open) or at high mass resolution (reduced slit width). For a more detailed overview of instrumentation, peculiarities and performance see Jakubowski *et al*. (1998).

The Pu measurements (reference date 1st October 2001) are traceable to two isotopic standard solutions. One was used to calibrate the ICP-SFMS, and is a standard of ^{239}Pu (reference no. E4310/98, 2.5 Bq g^{-1}±2.2% (2σ), obtained from the National Physical Laboratory (NPL), Teddington, Middlesex TW11 0LW, UK) utilized in a diluted form of 0.4 Bq g^{-1}. The other was a standard of ^{242}Pu (also obtained from NPL), used as a chemical separation yield tracer and derived

from a 0.2 Bq ml^{-1} solution of ^{242}Pu. A further standard of natural uranium was utilized to determine the extent of hydride generation interference with ^{239}Pu and ^{240}Pu measurements (reference NIST SRM 4321C, 242 Bq g^{-1} ^{238}U, prepared by the US National Institute of Standards).

Sample preparation and plutonium separation

The soil samples were air dried, gently disaggregated and sieved through a 2 mm plastic mesh to remove stones and fragments of plant roots. A 2 g ashed sample was weighed into a PTFE beaker, to which 15 ml of 12 M HCl and 3 ml of 16 M HNO_3 were added and allowed to reflux for 4 h at 150ºC. On cooling, the sample was filtered through a PTFE Millipore syringe filter and made up to volume in a 50 ml volumetric flask using 12 M HCl.

Specific preparative chemistry is required prior to measurement in order to separate the analyte of interest from other radioactive elements (e.g.^{238}U and ^{241}Am) and other potential interfering species (e.g. $^{238}U^{1}H^{+}$) (Bienvenu *et al*., 1998; Truscott *et al*., 2001). One ml of 16 M HNO_3 was added to each aliquot to control the Pu oxidation state to Pu(IV). The sample was then passed through a conditioned anion exchange column (depth 6 cm, Bio-Rad AG1-X8, 100−200 mesh). Pu is retained as the $PuCl_6^{2-}$ species. Iron, and selected actinides, were removed by washing with 20 ml of 9 M HCl, which removes Am, 25 ml of 8 M HNO_3, which removes Fe, and 25 ml 12 M HCl, which removes Th. Pu was then eluted with 25 ml of 11.5 M HCl/0.2 M HI and made up to 10 ml using 0.3 M HNO_3.

In order to determine the chemical recovery of Pu, the filtrate from the aqua-regia digestion procedure was split into two aliquots. The same separation procedure was followed for both aliquots. For each sample, one aliquot was spiked with a known activity of ^{242}Pu, which acts as the chemical yield tracer. This provided a measurement of the chemical yield of Pu (for the spiked aliquots only), and enabled quantitative determination of Pu isotopic content for the mass range 238−241 in the soil samples. The other aliquot was not spiked. This enabled a qualitative determination of the ^{242}Pu already present in the sample. The unspiked aliquot enabled us to confirm that no significant levels of ^{242}Pu were originally present in the samples (^{242}Pu elutent concentrations were <1% of the added chemical yield tracer; as seen in Table 2 discussed in detail below).

Measurement procedure and lower limits of detection

The Pu isotopic concentration of the elutant was then quantified using an ICP-SFMS. The system was calibrated using aliquots of the ^{239}Pu standard. The ^{239}Pu calibration standards were produced by dilutions in Milli-Q water (18 MΩcm), and acidified with 0.3 M aristar grade HNO_3.

Plutonium is present in Chernobyl fallout as five isotopes: ^{238}Pu, ^{239}Pu, ^{240}Pu, ^{241}Pu and ^{242}Pu (Boulyga *et al*., 2001). Hence, Pu isotopic measurements were undertaken for mass numbers 238−242 inclusive. The measurements for these mass numbers were corrected to eliminate instrumental drift. Hydride generation corrections were applied for mass numbers 239 and 240, by use of isotopic standards of ^{238}U and ^{239}Pu, as referenced above. These isotopic standards enabled determination of the extent of interference from $^{238}U\text{-}H^{+}$, $^{238}U\text{-}2H^{+}$ and $^{239}Pu\text{-}H^{+}$. The hydride generation correction to the mass 239 isobar count was 0.01% of the total count for the mass 238 isobar. The correction to the mass 240 isobar, due to single hydride formation, was 0.12% of the total count for the mass 239 isobar. Double hydride interference to the mass 240 isobar was found to be negligible.

Indicative lower limits of detection in soil (LLDs) using a procedural blank are given in Table 1 for mass isobars 238−242. The LLD is defined as three standard deviations of the measurement obtained from five sequential analyses of a representative procedural blank. Instrumental noise, contamination from reagents and the equipment utilized, results in some variability of LLDs determined using procedural blanks. The LLDs quoted in Table 1 are indicative of an achievable LLD in our soils using the procedure outlined above.

Table 1 gives the maximum allowable soil concentration (MAC) for each radioisotope as derived from the US EPA proposed annual effective dose equivalent limit of 0.15 mSv y^{-1} [US EPA (1997) from Wood *et al*., 1999)]. Exposure in excess of 0.15 mSv y^{-1} to any individual radioisotope listed in Table 1 indicates the presence of an environmentally significant level of radioactivity that would normally instigate clean-up procedures. As can be seen from Table 1, our detection limits for each of the

TABLE 1. Indicative lower limits of detection (LLD) in the soil determined using a representative procedural blank. The LLD is defined as three standard deviations of the measurement obtained from five sequential analyses of this blank. Maximum allowable soil concentrations (MAC) as Bq kg^{-1} are reported from Wood *et al*. (1999) and are based on the US EPA effective dose equivalent limit of 0.15 mSv y^{-1}.

Radionuclide	Half life (y^{-1})	Procedural blank LLD ppt (10^{-12})	LLD as Bq kg^{-1} in the soil	0.15 mSv MAC as Bq kg^{-1}
^{238}Pu	87.7	0.85	539	1202 (^{238}U = 196)
^{239}Pu	24110	0.051	0.12	1090
^{240}Pu	6563	0.016	0.13	1090
^{241}Pu	14.4	0.0052	19.9	285 (^{241}Am = 8)
^{242}Pu	373300	0.0043	0.00062	1145

Pu isotopes are significantly below the concentration levels of environmental concern.

Plutonium content in Belarus soil samples

In Table 2 we present the Pu isotopic content determined on soils from the three sampling locations (EZ, Vetka-C, Vetka-D). The Pu concentrations in all three soil profiles are at a maximum in the uppermost few centimetres, as expected for sites undisturbed since the Chernobyl accident. Measurement precision is quoted as % relative standard deviation (%RSD) of three sequential analyses of an aliquot. With the exception of two determinations, a precision of 1 to 15%RSD was achieved for the exclusion zone samples (EZ) across all five Pu isotopes (Table 2). For the Vetka samples (Vetka-C and D), a precision of ~1 to ~5%RSD was achieved for ^{238}Pu and ^{242}Pu. However, precisions for the isotopes ^{239}Pu, ^{240}Pu and ^{241}Pu were much more variable, and typically in the range ~10 to ~30%RSD (Table 2).

The % recovery of the ^{242}Pu chemical yield tracer (Table 2) varied with soil textural class. The sandy soils from site EZ indicated a % recovery ranging from 91.3 to 105.6% (i.e. ±7.15%); the sandy-loam soils from site Vetka-C ranged from 105−123% (i.e. ±9.00%), whilst the organic soils from Vetka-D ranged from 73.2 to 89.5% (i.e. ±8.15%; the lowermost sample (34−36 cm) is excluded from this range since it was more minerogenic in nature, and hence a different textural class). The % recoveries in excess of 100% are difficult to explain. A detailed review of our analytical and measurement procedures (e.g. inaccuracy in the dilution and dispensing of the certified activity ^{242}Pu yield tracer; procedural contamination during the sequential separation procedure) did not indicate any errors or contamination that might lead to an increased count rate for the mass 241. Given the apparently erroneous count rate for the mass 242 only occurs in the samples containing soil (specifically the sandy-loam soils of site Vetka-C), interferences occurring due to the presence of the soil matrix would seem to be the most likely suggestion. Possible interfering complexes may include $^{226}Rn^{16}O$ and $^{210}Pb^{32}S$ which if present would occur at the same nominal mass as ^{242}Pu. This problem of recoveries in excess of 100% cannot be explained at this time and is the focus of current work.

The isotopic concentrations given in Table 2 have been converted to specific activity (Bq kg^{-1}; Table 3), to aid comparison with the MACs calculated by Wood *et al*. (1999; Table 1). The surprisingly high ^{238}Pu specific activities (Table 3; MAC of 1202 Bq kg^{-1}), in all of the samples, suggests that a proportion of ^{238}U must have 'leaked' through the sequential separation procedure. This is further supported by the lack of correlation between the ^{238}Pu and the ^{239}Pu measurements. The typical concentration of 'natural' U in soil is ~1 mg kg^{-1} (Alloway, 1995). The residual concentration of ^{238}U inferred to be present in these samples would therefore be considerably <1% of the typical natural concentration. So, a significant proportion of the naturally occurring ^{238}U must have been removed by the sequential separation procedure. Thus, ICP-SFMS can be applied to confirm levels of ^{238}Pu, below levels of MAC, only if separation can eliminate ^{238}U to levels below 1 part per

TABLE 2. Soil Pu concentrations for mass numbers 238–242 inclusive, quoted to 3 significant figures, and the $^{240}Pu/^{239}Pu$ ratio, for Chernobyl fallout-contaminated soils from sampling sites EZ (exclusion zone) and Vetka (C and D).

	Aliquot/ spiked/ non spike	Pu 242 spike (pbb)	Chemical yield for Pu spike (%)	Pu (U) 238 (ppb)	Pu 239 (ppb)	Pu 240 (ppb)	Pu 241 (ppb)	240/239
	Spiked	0.0534		0.124	0.00683	0.00278	0.475	0.41
EZ (0–2 cm)		%RSD = 1.50	98.9	%RSD =6.25	%RSD = 3.33	%RSD = 1.18	%RSD = 11.0	±4.5%
	Non spiked	0.000227 %RSD = 9.21		0.106 %RSD = 0.963	0.00721 %RSD = 4.14	0.00312 %RSD = 2.06	0.479 %RSD = 10.3	0.43 ±6.2%
	Spiked	0.0544		0.118	0.00586	0.00233	0.458	0.40
EZ (2–4 cm)		%RSD = 1.30	101	%RSD = 4.34	%RSD = 1.95	%RSD = 2.75	%RSD = 11.5	±4.7%
	Non spiked	0.000147 %RSD = 16.9		0.117 %RSD = 1.59	0.00665 %RSD = 5.36	0.00264 %RSD = 3.31	0.467 %RSD = 13.5	0.40 ±8.7%
	Spiked	0.0493	91.3	0.073	0.000666	0.000307	0.0606	0.46
EZ (4–6 cm)		%RSD = 1.31		%RSD = 3.13	%RSD = 1.00	%RSD = 3.45	%RSD = 0.76	±4.5%
	Non spiked	0.0000214 %RSD = 0.444		0.093 %RSD = 4.56	0.000681 %RSD = 2.33	0.000295 %RSD = 7.50	0.0713 %RSD = 3.35	0.43 ±9.8%
	Spiked	0.0514		0.089	0.000278	0.000133		0.48
EZ (8–10 cm)		%RSD = 0.321	95.2	%RSD = 2.43	%RSD = 1.20	%RSD = 10.4	<LLD	±11.6%
	Non spiked	<LLD		0.104 %RSD = 3.69	0.000313 %RSD = 6.51	0.000139 %RSD = 15.1	0.00837 %RSD = 0.66	0.44 ±21.6%
	Spiked	0.0570		0.097				
EZ (34–36 cm)		%RSD = 1.47	105.6	%RSD = 4.24	<LLD	<LLD	<LLD	n.a.
	Non spiked	<LLD		0.134 %RSD = 2.64	<LLD	<LLD	<LLD	n.a.
	Spiked	0.0308		0.397	0.000126	0.0000329		0.26
Vetka-C (0–2 cm)		%RSD = 7.23	114	%RSD = 3.70	%RSD = 26.0	%RSD = 15.7	<LLD	±41.7%
	Non spiked	<LLD		0.445 %RSD= 2.58	0.000155 %RSD = 27.4	0.0000304 %RSD = 50.8	<LLD	0.20 ±78.2%
	Spiked	0.0316		0.375	0.0000619	0.0000224		0.36
Vetka-C (2–4 cm)		%RSD = 2.61	117	%RSD = 1.47	%RSD = 31.7	%RSD = 22.1	<LLD	±53.8%
	Non spiked	<LLD		0.352 %RSD= 5.78	<LLD	<LLD	<LLD	n.a.
	Spiked	0.0283		0.296	0.0000488	0.0000255		0.52
Vetka-C (4–6 cm)		%RSD = 1.63	105	%RSD = 2.02	%RSD = 20.7	%RSD = 9.57	<LLD	±30.8%
	Non spiked	–	–	–	–	–	–	
	Spiked	0.0333		0.338		0.0000116		
Vetka-C (8–10 cm)		%RSD = 2.22	123	%RSD = 0.513	<LLD	%RSD = 14.5	<LLD	n.a.
	Non spiked	–	–	–	–	–	–	

TABLE 2 (*contd.*). Soil Pu concentrations for mass numbers 238–242 inclusive, quoted to 3 significant figures, and the $^{240}Pu/^{239}Pu$ ratio, for Chernobyl fallout contaminated soils from sampling sites EZ (exclusion zone) and Vetka (C and D).

	Aliquot/ spiked/ no spike	Pu 242 spike (pbb)	Chemical yield for Pu spike (%)	Pu (U) 238 (ppb)	Pu 239 (ppb)	Pu 240 (ppb)	Pu 241 (ppb)	240/239
	Spiked	0.0302	112	0.285	<LLD	<LLD	<LLD	n.a.
Vetka-C (34–36 cm)		%RSD = 1.83	–	%RSD = 1.84				
	Non spiked	0.0000093 %RSD = 59.4	–	0.3972 %RSD = 2.56	<LLD	<LLD	<LLD	n.a.
	Spiked	0.0242		1.98	0.000202	0.0000767		0.38
Vetka-D (0–2 cm)		%RSD = 5.65	89.5	%RSD = 4.98	%RSD = 6.09	%RSD = 18.1	<LLD	±24.2%
	Non spiked	0.00000722 %RSD = 0.260	–	2.22 %RSD = 0.927	0.000156 %RSD= 25.0	0.0000778 %RSD= 68.5	<LLD	0.50 ±93.5%
	Spiked	0.0213		2.46	0.000126	0.0000498		0.40
Vetka-D (2–4 cm)		%RSD = 0.95	79.1	%RSD = 0.654	%RSD = 8.96	%RSD = 31.1	<LLD	±40.0%
	Non spiked	<LLD	–	2.46 %RSD = 0.497	0.000172 %RSD= 17.3	0.0000636 %RSD= 18.9	<LLD	0.37 ±36.2%
Vetka-D (6–8 cm)	Spiked	0.0198 %RSD = 1.88	73.2	3.017 %RSD = 1.72	0.0000416 %RSD = 37.9	0.0000214 %RSD = 84.9	<LLD	0.51 ±122.8%
	Non spiked	–	–	–	–	–	–	
Vetka-D (34–36 cm)	Spiked	0.0278 %RSD = 2.27	103	0.500 %RSD = 1.08	<LLD	<LLD	<LLD	n.a.
	Non spiked	<LLD	–	0.710 %RSD= 1.90	<LLD	<LLD	<LLD	n.a.

<LLD denotes below the lower limit of detection. The % chemical yield of the ^{242}Pu spike is also indicated.

million of the original concentration (i.e. 99.9999% removal of ^{238}U). Given this potential masking of ^{238}Pu, these data are not considered further here.

The sequential chemical separation procedure, followed by ICP-SFMS, can also leave an ambiguity as to the elemental nature of the radiological hazard from the mass 241 isobar. This can arise if the sequential separation procedure does not remove all of the Am. This ambiguity relates to the EZ samples where mass 241 has been identified. The Vetka samples yielded mass 241 concentrations below our detection limits and hence are not discussed further here. Further work, using gamma spectroscopy, is required to clarify the extent to which any ^{241}Am may have 'leaked' through the sequential chemical separation procedure. However, predictions of the $^{241}Pu/^{241}Am$ ratio at the time of the Chernobyl accident may be used to quantify a potential maximum activity of ^{241}Am in the soil samples. Calculation of the current $^{241}Pu/^{241}Am$ activity ratio, as at 1/10/02, was based on the assumption that at the time of the accident, radioactive fallout was deposited at site EZ in the same ratio as in the core inventory. This calculation also assumes no isotopic fractionation and a closed system following deposition. Based on estimates of the core inventory by Kirchner and Noack (1988) the current (1/10/02) activity ratio of $^{241}Pu/^{241}Am$, in the soil samples, is 26:1. This calculation accounts for the presence of ^{241}Pu and ^{241}Am not in equilibrium. Assuming that the sequential separation procedure eliminated all of the ^{241}Am, and hence the ICP-SFMS measurement of mass 241 relates only to ^{241}Pu present in the sample, then a maximum presence of 70 Bq $^{241}Am\ kg^{-1}$ might be expected in the

TABLE 3. Soil Pu concentrations presented as specific activity (Bq kg^{-1}) (reference date 1st October 2001). The %RSDs of these measurements are given in Table 2. The half lives used in the conversion of ppb and ppt to Bq kg^{-1} are given in brackets beneath the relevant isotope.

	^{242}Pu (373300 y)	^{238}Pu (87.7 y)	^{238}U (4.5E+09 y)	^{239}Pu (24110 y)	^{240}Pu (6563 y)	^{241}Pu (14.35 y)
EZ (0–2 cm)	0.0334	78610	0.00153	16.6	23.3	1820
EZ (2–4 cm)	0.0216	74800	0.00146	13.4	19.5	1750
EZ (4–6 cm)	0.000313	46280	0.000902	1.53	2.58	232
EZ (8–10 cm)	<LLD	56420	0.00110	0.638	1.12	<LLD
EZ (34–36 cm)	<LLD	61490	0.00120	<LLD	<LLD	<LLD
Vetka-C (0–2 cm)	<LLD	251700	0.00490	0.289	0.277	<LLD
Vetka-C (2–4 cm)	<LLD	237700	0.00463	0.142	0.185	<LLD
Vetka-C (4–6 cm)	<LLD	187600	0.00366	0.112	0.214	<LLD
Vetka-C (8–10 cm)	<LLD	214270	0.00418	<LLD	0.097	<LLD
Vetka-C (34–36 cm)	<LLD	180670	0.00352	<LLD	<LLD	<LLD
Vetka-D (0–2 cm)	0.00116	1256400	0.02449	0.464	0.647	<LLD
Vetka-D (2–4 cm)	<LLD	1558800	0.03038	0.289	0.418	<LLD
Vetka-D (6–8 cm)	<LLD	191250	0.03727	0.0964	0.180	<LLD
Vetka-D (34–36 cm)	<LLD	317000	0.00618	<LLD	<LLD	<LLD

<LLD denotes below the lower limit of detection. The concentrations at isobar 238 have been converted to activity using the half life of ^{238}Pu and ^{238}U.

soil samples, based on our measured ^{241}Pu content of 1820 Bq kg^{-1} (EZ, 0–2 cm; Table 3). Hence, the ^{241}Pu and ^{241}Am specific activities for site EZ, determined on the basis of counts for the 241 mass isobar arising entirely from ^{241}Pu, both yield values in excess of MAC (Table 3; ^{241}Pu MAC = 285 Bq kg^{-1}; ^{241}Am MAC = 8 Bq kg^{-1}).

The relative isotopic abundances of Pu vary with the source from which they originate (i.e. the source term) and the subsequent irradiation history of the material. For environmental monitoring in the vicinity of nuclear facilities, the ^{240}Pu/^{239}Pu isotope ratio is of importance because it can provide information on the source of the contamination (Rodushkin *et al*., 1999). In contrast with the difficulty of distinguishing between ^{240}Pu and ^{239}Pu by alpha spectrometry, ICP-SFMS readily differentiates these radioisotopes and hence provides ratio values. ^{239}Pu is present in weapons-grade Pu at high abundance relative to ^{240}Pu (^{240}Pu /^{239}Pu characteristically $\approx$0.05; Taylor *et al*., 2001). After detonation, this ratio increases (due to neutron capture) and the ^{240}Pu/^{239}Pu ratio in weapons test fallout varies between 0.10 and 0.35, with an average of ~0.18 (Koide *et al*., 1985). For reactor-grade Pu, the ^{240}Pu/^{239}Pu ratio can vary from 0.06 to 0.65 depending on the irradiation conditions of the fuel (Rodushkin *et al*., 1999). Typical ratios in mixed oxide fuel are ~0.4.

On the basis of the Chernobyl core inventory estimates for ^{240}Pu and ^{239}Pu by Begichev *et al*. (1989) and Sich (1993), a ratio of ~0.43 is expected in Chernobyl-derived fallout. Table 2 indicates the ^{240}Pu/^{239}Pu ratio for each of the spiked and non-spiked samples. The EZ samples indicate a ratio of 0.40 to 0.48, which agrees well with the expected ratio for isotopes arising from the Chernobyl core and ratios for Chernobyl fuel (0.42; Begichev *et al*., 1990). The very low activities of ^{239}Pu and ^{240}Pu identified at Vetka-C and Vetka-D resulted in experimental errors for this ratio all in excess of ±30% (Table 2). Given the large uncertainties associated with these ratios, any interpretation will be ambiguous; however, ^{240}Pu/^{239}Pu ratios of ~0.33 have been measured in the vicinity of Chernobyl (Boulya *et al*., 1997). This ratio is in reasonable agreement with several of our Vetka ratios.

The low concentrations of Pu in this location are indicative of being primarily derived from global fallout following atmospheric nuclear tests in the 1960s. The cumulative deposition of ^{239,240}Pu in the northern hemisphere from atmospheric nuclear tests has been reported to be in the order of 58 Bq m^{-2} (UNSCEAR, 1982). Whilst Hoygle and Maly (2000) observe values ranging from 49.32 Bq m^{-2} to 55.01 Bq m^{-2} in the Czech Republic. Our data for Vetka-C indicate a cumulative ^{239,240}Pu deposition in the order of 37 Bq m^{-2}, which is comparable to global fallout values, given the non-uniformity of weapons fallout deposition.

Whereas the Vetka-C and D locations contain levels of fission products comparable to those found at the EZ site, they contrast with the EZ site in having only low levels of Pu isotopes. The specific activities of Pu at sites C and D are well below MACs. We find no evidence for significant levels of Pu-bearing fuel particulates at the Vetka sites.

Conclusion

A range of instrumental techniques is required to characterize hot-particle presence in soil. Gamma spectroscopic and autoradiographic techniques provide unambiguous indications of the presence of hot particles and a quantification of the magnitude of presence of the most significant fission product radioisotopes namely ^{137}Cs (by gamma spectroscopy) and ^{90}Sr (by autoradiography). We show how differential autoradiographic imaging (DAI) enables the non-destructive isotopic classification of radioactive contamination in soil and how ICP-SFMS may provide supplementary information on the presence of transuranic actinides. An analytical method for the isotopic analysis of Pu in soil samples using ICP-SFMS is described, with detection limits in the sub-ppt (10^{-12}) range. Determination of Pu at trace and ultratrace concentrations is of importance due to the radiotoxicity of this element.

Our characterization of the hot-particle content in one location near to the Chernobyl reactor (site EZ) and two other locations 170 km from the reactor (Vetka-C and Vetka-D) show widely contrasting fallout characteristics. The nearer site is rich in Cs- and Sr-bearing particles, present at levels of several hot particles per gram. We estimate the hot-particle content to comprise ~5000 particles per kg, with an average activity of 20 Bq per particle. These particulates are likely to be primarily associated with reactor fuel, a conclusion that links well with an observed ^{240}Pu/^{239}Pu ratio of 0.4 to 0.48. This is in accordance with Pu derived from the reactor core. As expected, the hazardous nature of this site is indicated by the high specific activities observed by gamma spectroscopy. Additionally ^{241}Pu and the inferred ^{241}Am concentrations are far in excess of the MAC (after Wood *et al*., 1999). This abundance of heavy radionuclides, and the large hot-particle content, will negate land rehabilitation over many hundreds of years.

At the Vetka site, we confirm the expectation that lower levels of hot particles are present in the soil. There is no evidence for the presence of Pu in excess of global atmospheric fallout levels. The results are encouraging for the future rehabilitation of the Bryansk-Belarus spot where the radiological hazard, including hot-particle content, is dominated by fission products with half-lives in the region of 30 years. Here, it may be possible for abandoned areas to be returned to agricultural use and habitation over the next few decades.

Acknowledgements

The authors are indebted to colleagues at the International Sakharov Environmental University, Minsk, Belarus. Without their support and enthusiasm, the field sampling programmes would not have been possible. In particular, we would like to acknowledge the expertise and assistance of Dr Sergei Zenchenko and Dr

Alexander Milutin, as well as Galina and Roman from the International office. Additional thanks must also go to Olivia Marsden (University of Manchester) and Dr John Williams (Nu Instruments, Wrexham) for guidance with the sequential separation procedure and the Axiom, respectively. The valuable comments made on an earlier draft of this paper by Karen Hudson-Edwards and two anonymous referees are gratefully acknowledged.

References

Adams, C.E., Farlow, N.H. and Shell, W.R. (1960) The composition structures and origins of radioactive fallout particles. *Geochemica et Cosmochemica Acta*, **18**, 42–56.

Alloway, B.J. (1995) *Heavy Metals in Soils*, 2nd edition. Blackie, London.

Begichev, S.N., Borovi, A.A., Burlakov, E.V., Gagrinsky, A.Ju., Demin, V.F., Khodakovsky, I.L. and Khrulev, A.A. (1989) Radioactive releases due to the Chernobyl accident. *Presented at the International Seminar on Fission Product Transport Processes in Reactor Accidents*, 22–26 May, 1989, Dubrovnik, Yugoslavia.

Begichev, S.N., Borovoj, A.A., Burlakov, E.B., Gararinsky, A.J., Denim, V.F., Khrulev, A.A. and Khodakovsky, I.L. (1990) Radioactive releases due to the Chernobyl accident. Pp. 717–734 in: *Fission Product Transport Processes in Reactor Accidents* (J.T. Rogers, editor). Hemisphere Publishing, USA.

Belli, M. and Tikhomirov, F., editors (1996) *Experimental Collaboration Project Number 5*. European Community, Brussels.

Bienvenu, P.G., Brochard, E.A. and Excoffier, E.A. (1998) Determination of long-lived beta emitters in nuclear waste by inductively coupled plasma-mass spectrometry. Pp. 51–63 in: *Applications of Inductively Coupled Plasma-Mass Spectrometry to Radionuclide Determination* (R.W. Morrow and J.S Crain, editors). ASTM, Pennsylvania, USA

Bogatov, S., Borovoj, A., Dubasov, Yu. and Lomonosov, V. (1990) Forms and characteristics of hot particles of fuel at the Chernobyl NPP accident. *Atomnaya Energiya*, **69**, 36–40.

Bolsunovsky, A.Ya. and Tcherkezian, V.O. (2001) Hot particles of the Yenisei River flood plain, Russia. *Journal of Environmental Radioactivity*, **57**, 167–174.

Bondarenko, O.A., Salmon, P.L., Henshaw, D.L., Fews, A.P. and Ross, A.N. (1996) Alpha-particle spectroscopy with Tastrak (CR-39) type plastic, and its application to the measurement of hot particles. *Nuclear Instruments and Methods in Physics Research A*, **369**, 582–587.

Boulya, S.F., Erdmann, N., Funk, H., Kievets, K., Lomonosova, E.M., Mansel, A., Trautmann, N., Yaroshevich, O.I. and Zhuk, I.V. (1997) Determination of isotopic composition of Pu in hot particles of the Chernobyl area. *Radiation Measurements*, **28**, 349–352.

Boulyga, S.F., Testa, C., Desideri, D. and Becker, S.J. (2001) Optimisation and application of ICP-MS and alpha-spectrometry for determination of isotopic ratios of depleted uranium and plutonium in samples collected in Kosovo. *Journal of Analytical Atomic Spectrometry*, **16**, 1283–1289.

Broda, R., Kubica, B., Szeglowski, Z. and Zuber, K. (1989) Alpha emitters in Chernobyl hot particles. *Radiochimica Acta*, **48**, 89–96.

Bunzl, K. (1997) Probability for detecting hot particles in environmental samples by sample splitting. *Analyst*, **122**, 653–656.

Bunzl, K. (1998) Detection of radioactive hot particles in environmental samples by repeated mixing. *Applied Radiation Isotopes*, **49**, 1625–1631.

Charles, M.W. (1991) The hot particle problem. *Radiation Protection Dosimetry*, **39**, 39–47.

Chevchuka, V.E. and Gurachevsky, V.L. (2001) *15 Years After the Chernobyl Accident*. State Committee on Post-Chernobyl Problems, Republic of Belarus, Minsk.

Edvarson, K., Low, K. and Sisefsky, J. (1959) Fractionation phenomena in nuclear weapons debris. *Nature*, **184**, 1771–1774.

Hoygle, Z. and Maly, M. (2000) Sources, vertical distribution, and migration rates of ^{239,240}Pu, ^{238}Pu, and ^{137}Cs in grassland soil in three localities of central Bohemia. *Journal of Environmental Radioactivity*, **47**, 135–147.

Jakubowski, N., Moens, L. and Vanhaecke, F. (1998) Sector field mass spectrometers in ICP-MS. *Spectrochimica Acta*, **53**, 1739–1763.

Kirchner, G. and Noack, C.C. (1988) Core history and nuclide inventory of the Chernobyl core at the time of the accident. *Nuclear Safety*, **29**, 1–5.

Koide, M., Bertine, K.K., Chow, T.J. and Goldberg, E.D. (1985) The Pu-240 Pu-239 ratio, a potential geochronometer. *Earth and Planetary Science Letters*, **72**, 1–8

Krouglov, S.V., Filipas, A.S., Alexakhin, R.M. and Arkhipov, M.N.P. (1997) Long-term study on the transfer of 137Cs and 90Sr from Chernobyl-contaminated soils to grain crops. *Journal of Environmental Radioactivity*, **34**, 267–286.

Larsen, I.L., Lee, S.Y., Boston, H.L. and Stetar, E.A., (1992) Discovery of a 137Cs hot particle in municipal wastewater treatment sludge. *Health Physics*, **62**, 235–238.

Longworth, G., Carpenter, B., Bull, R., Toole, J. and Nichols, A. (1998) *The Radiochemical Manual*.

AEA Technology Plc, Oxford, UK.

Mamuro, T., Fujita, A. and Matsunami T. (1965) Microscopic examination of highly radioactive fallout particles from the first Chinese nuclear test explosion. *Health Physics*, **11**, 1097–1101.

Mandjoukov, I.G., Burin, K., Mandjoukova, B., Vapirev, E.I. and Tsacheva, T. (1992) Spectrometry and visualization of 'standard' hot particles from the Chernobyl accident. *Radiation Protection Dosimetry*, **40**, 235–244.

Morrow, R.W. and Crain, J.S., editors (1998) *Applications of Inductively Coupled Plasma-Mass Spectrometry to Radionuclide Determinations*. ASTM, USA.

Nageldinger, G. (1998) *Characterisation of Chernobyl fallout in Belarus soil*. Ph.D. thesis, Kingston University, Surrey, UK.

Nageldinger, G., Flowers, A., Schwerdt, C. and Kelz, R. (1998*a*) Autoradiographic film evaluated with desk-top scanner. *Nuclear Instruments and Methods in Physics Research A*, **416**, 516–524.

Nageldinger, G., Flowers, A., Henry, B. and Postaul, J. (1998*b*) Hot particle detection using uncertainties in activity measurements of soil. *Health Physics*, **74**, 472–477.

Nageldinger, G., Flowers, A. and Entwistle, A. (1999) A new mechanism for hot particle development in soil following ionic contamination with radiocesium. *Health Physics*, **75**, 646–647.

Organisation for Economic Cooperation and Development (OECD) (1995) *The Radiological and Health Impact of Chernobyl*. OECD Nuclear Energy Agency, USA.

Osuch, S., Dabrowska, M., Jaracz, P., Kaczanowski, J., Van Khoi, L., Mirowski, S., Piasecki, E., Szeflinska, Z., Tropilo, J. and Wilhelmi, Z. (1989) Isotopic composition of high-activity particles released in the Chernobyl accident. *Health Physics*, **57**, 707–716.

Philipsborn, H. and Steinhaeusler, F. (1988) Hot particles from the Chernobyl fallout. *Proceedings of an International Workshop held in Theuern*, 28–29 October, 1987.

Pollanen, R. and Torvonen, H. (1994*a*) Skin doses from large uranium fuel particles – application to the Chernobyl accident. *Radiation Protection Dosimetry*, **54**, 127–132.

Pollanen, R. and Toivonen, H. (1994*b*) Transport of large uranium fuel particles released from a nuclear power plant in a severe accident. *Journal of Radiological Protection*, **14**, 55–65.

Pollanen, R., Valkama, I. and Toivonen, H. (1997) Transport of radioactive particles from the Chernobyl accident. *Atmospheric Environment*, **31**, 3575–3590.

Powers, D.A., Kress, T.S. and Jankowski, M.W. (1987) The Chernobyl source term. *Nuclear Safety*, **28**, 10–28.

Rodushkin, I., Linahl, P., Holm, E. and Roos, P. (1999) Determination of plutonium concentrations and isotope ratios in environmental samples with a double-focusing sector field ICP-MS. *Nuclear Instruments and Methods in Physics Research A,* **423**, 472–479.

Salbu, B. (2000) Source-related characteristics of radioactive particles: a review. *Radiation Protection Dosimetry*, **92**, 49–54.

Sandalls, F.J., Segal, M.G. and Victorova, N. (1993) Hot particles from Chernobyl: a review. *Journal of Environmental Radioactivity*, **18**, 5–22.

Sanzharova, N.I., Fensenko, S.V., Kotik, V.A. and Spiridonov, S.I. (1996) Behaviour of radionuclides in meadows and efficiency of countermeasures. *Radiation Protection Dosimetry*, **64**, 43–48.

Sich, A.R. (1993) *The Chernobyl accident revisited: source term analysis and reconstruction of events during the active phase*. Ph.D. thesis, Massachusetts Institute of Technology, USA.

Taylor, R.N., Warneke, T., Milton, A., Croudace, I.W., Warick, P.E. and Nesbitt, R.W. (2001) Plutonium isotope ratio analysis at femtogram to nanogram levels by multicollector ICP–MS. *Journal of Analytical Atomic Spectrometry*, **16**, 279–284.

Tcherkezian, V., Shkinev, V., Khitro, L. and Kolesov, G. (1994) Experimental approach to Chernobyl hot particles. *Journal of Environmental Radioactivity*, **22**, 127–139.

Truscott, J.B., Jones, P., Fairman, B.E. and Evans, E.H. (2001) Determination of actinide elements at femtogram per gram levels in environmental samples by on-line solid phase extraction and sector field inductively coupled plasma-mass spectrometry. *Analytica Chimica Acta*, **433**, 245–253.

UNSCEAR (1982) *Ionising Radiation and Biological Effects*. United Nations, New York, USA.

U.S. Environmental Protection Agency (1997) *Establishment of cleanup levels for CERCLA sites with radioactive contamination*. OSWER 9200, United States Environmental Protection Agency, Washington D.C.

Victorova, N.V. and Garger, E.K. (1990) Investigations of the deposition and spread of radioactive aerosol particles in the Chernobyl zone based on biological monitoring. Pp. 223–236 in: *Proceedings Report EUR 13574*. Commission of the European Communities, Luxembourg.

Wood, J.L., Benke, R.R., Rohrer, S.M. and Kearfott, K.J. (1999) A comparison of minimum detectable and proposed maximum allowable soil concentration clean-up levels for selected radionuclides. *Health Physics*, **76**, 413–417.

Zheltonozhsky, V., Muck, K. and Bondarkov, M. (2001) Classification of hot particles from the Chernobyl

accident and nuclear weapons detonations by non-destructive methods. *Journal of Environmental Radioactivity*, **57**, 151–166.

[*Manuscript received 20 March 2002: revised 27 August 2002*]